

# A cortical locus for the processing of contrast-defined contours

Isabelle Mareschal and Curtis L. Baker, Jr.

McGill Vision Research Unit, Department of Ophthalmology, 687 Pine Avenue West H4-14, Montreal, Quebec H3A 1A1, Canada  
Correspondence should be addressed to I.M. ([Isabelle@astra.vision.mcgill.ca](mailto:Isabelle@astra.vision.mcgill.ca))

Object boundaries in the natural environment are often defined by changes in luminance; in other cases, however, there may be no difference in average luminance across the boundary, which is instead defined by more subtle 'second-order' cues, such as changes in the contrast of a fine-grained texture. The detection of luminance boundaries may be readily explained in terms of visual cortical neurons, which compute the linear sum of the excitatory and inhibitory inputs to different parts of their receptive field. The detection of second-order stimuli is less well understood, but is thought to involve a separate nonlinear processing stream, in which boundary detectors would receive inputs from many smaller subunits. To address this, we have examined the properties of cortical neurons which respond to both first- and second-order stimuli. We show that the inputs to these neurons are also oriented, but with no fixed orientational relationship to the neurons they subserve. Our results suggest a flexible mechanism by which the visual cortex can detect object boundaries regardless of whether they are defined by luminance or texture.

The selectivity with which visual cortical neurons respond to stimulus attributes such as orientation and spatial frequency has been understood largely in terms of a linear summation of local luminance levels over their receptive fields<sup>1-4</sup>. In this scheme, a receptive field has spatially segregated excitatory and inhibitory regions whose inputs cancel out when equally stimulated. This idea is illustrated in Fig. 1a, where the luminance sinewave grating is optimally positioned to stimulate the receptive field shown. In addition, many cells exhibit selectivity to the direction and speed of motion of the stimulus; this could be explained by different regions of the receptive field exhibiting different response latencies, such that synchronous response summation will only occur when the stimulus moves at a velocity matched to the change of latency with position<sup>5</sup>. Because the stimulus selectivity of such neurons can be understood in terms of the spatial and temporal structure of their receptive fields, they have been likened to linear signal-processing filters. They may also correspond to the psychophysically defined filters that have been invoked in models of motion processing<sup>6-8</sup>.

However, some cortical neurons show response characteristics which cannot be explained by a simple summation scheme. One example is a stimulus consisting of a fine-grained texture (referred to as the 'carrier') whose contrast varies so as to define a spatial pattern (the 'envelope'). Because the light and dark texture elements are much smaller than the neuron's receptive field summation regions, they should cancel out within the individual excitatory and inhibitory regions (Fig. 1b). Because the mean luminance of the excitatory and inhibitory regions is the same, any response to the contrast-defined envelope ('second-order' stimulus) cannot be accounted for by linear summation<sup>9,10</sup>.

Recently, neurons in both the cat and macaque visual cortex have been discovered that respond selectively to boundaries of specific orientations, regardless of whether they are defined by first- or second-order cues<sup>11-13</sup>. Neurons have also been reported in the visual cortex that respond selectively to the orientation

of 'illusory contours'<sup>14,15</sup>. These findings provide support for the notion of 'form-cue invariance', whereby the accurate perception of a stimulus is largely independent of the physical cues defining it<sup>11</sup>. Such neurons may have an important functional role in the perception of natural scenes, where luminance-based cues are not useful, such as in breaking camouflage of textured objects or representing transparency<sup>16,17</sup>.

The detection of second-order stimuli cannot be accounted for by a simple distortion of the stimulus (e.g. via the retina), which could transform the original signal by, for example, unequally weighting the contribution of light and dark elements of the texture<sup>13,18,19</sup>. Instead their detection has been explained by two processing streams acting in parallel and converging onto the detectors that could mediate form-cue invariance. Luminance-defined stimuli are processed by a conventional linear stream, and second-order stimuli are processed by a nonlinear stream consisting of a 'filter-rectify-filter' cascade (e.g. Fig. 1c). In the nonlinear stream, the first-stage filters are tuned to the spatial scale of the carrier, their outputs undergo a nonlinearity (e.g. rectification) and are subsequently processed by a second linear filter, tuned to a coarser spatial scale<sup>13,20,21</sup>. Rectification can be likened to taking the absolute value of the positive and negative deviations from the average luminance of an image, a process that introduces a signal of a similar waveform as the contrast envelope. Although models of this class can account for much psychophysical<sup>22,23</sup> and physiological<sup>13,18</sup> data, the two-dimensional spatial relationship of the first- and second-stage filters, as well as their location in the visual system (e.g. cortical or sub-cortical), is unclear and is the motivation for our study.

Examples of first- and second-order stimuli used in these experiments are shown in Fig. 1a and b with a schematized neuron's receptive field superimposed. The luminance-defined sinewave grating is optimally matched to the neuron's receptive field (Fig. 1a) and should elicit a vigorous response. In this example, the second-order envelope stimulus in Fig. 1b consists of a

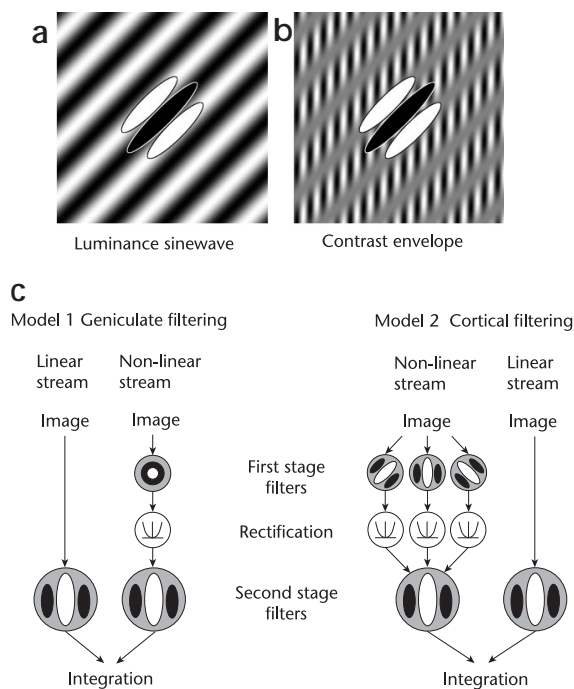


**Fig. 1.** Characteristics and processing of first- and second-order stimuli. **(a)** One frame of a first-order, luminance sinewave grating with a superimposed cartoon receptive field. The spatial frequency and orientation of the stimulus optimally matches the neuron's receptive field. **(b)** One frame of a second-order envelope stimulus. The carrier is vertical and of a high spatial frequency, whereas the envelope is oriented at 45° and at a lower spatial frequency. Notice that the gray levels falling in both excitatory and inhibitory regions of the receptive field average to zero (mid-gray). If the cell's receptive field summed linearly, then no response would be expected. **(c)** Two variations of 'two-stream models' to account for the processing of second-order stimuli. The processing of envelope stimuli should be independent of the carrier orientation in Model 1 but not in Model 2. In either case, the second-stage filters have spatial characteristics somewhat similar to the filters in the linear stream<sup>34</sup>.

stationary, vertical, high-spatial-frequency sinewave grating (carrier), whose contrast is modulated by a drifting 45°, low-frequency grating (envelope). Because the carrier is of a finer spatial grain than the receptive field, the average luminance of the envelope stimulus is the same across both inhibitory and excitatory regions. Nevertheless, neurons have been found that respond selectively to such envelope stimuli<sup>13,18</sup>.

Two variations of two-stream models that might account for responses to second-order stimuli are schematized in Fig. 1c. In both cases, the nonlinear stream has first-stage filters with excitatory and inhibitory summation regions much smaller than the second-stage ones; however the models differ in the degree to which the first-stage filters are tuned to orientation. In Model 1, the first-stage filters are non-oriented (isotropic), such that the envelope stimulus would elicit a response irrespective of the orientation of the carrier<sup>24</sup>. Model 2 uses oriented first-stage filters and predicts a strong dependence on the carrier orientation. There is accumulating psychophysical evidence that the first-stage filters are oriented<sup>21,25</sup>; however, the orientational relationship to the second stage filter is unclear. Some results support the

notion that the first-stage filters are predominantly of the same orientation as the second-stage filter<sup>25</sup>, whereas other findings suggest orthogonal inputs<sup>21</sup>. In the instance of the second model depicted here, we postulate that differently weighted, oriented first-stage filters feed into the second-stage filter.

Comparison of these models highlights two issues: whether the first-stage filters are oriented (and thus likely to be located in the cortex), and if so, whether there is a fixed orientational relationship between the first- and second-stage filters. Insight into the structure of the nonlinear stream is critical for the development of both physiological and psychophysical experiments to better understand how complex natural images are processed. In order to resolve these issues, we identified 24 neurons in cat area 18 (analogous to primate V2) that responded to both luminance and second-order contours. We examined the responses of these cells to envelope stimuli, as a function of both envelope and carrier orientation. The orientation tuning for envelope stimuli tended to be very similar to the tuning for first-order luminance stimuli. Responses to the envelope were also tuned with respect to carrier orientation, but we found no systematic relationship between the preferred orientations for the envelope and the carrier.

## Results

Figure 2 displays polar plots of normalized orientation responses, for three typical envelope-responsive neurons, to oriented stimuli moving in the preferred and null directions. Figure 2a shows the responses to coarse drifting sinewave gratings, defined by luminance alone. The neurons are clearly tuned for both the orientation and direction of these first-order stimuli. Figure 2b depicts responses to drifting envelope stimuli of different orientations, with the carrier fixed at the same orientation that was previously found to be optimal for the (much coarser) first-order stimulus (note that the carrier itself was stationary and, as such, would evoke no response in the absence of the envelope) and the envelope orientation varied. In Fig. 2c, the envelope orientation was fixed at the measured optimum, and the orientation of the carrier was varied. Insets of the stimuli indicating how the different parameters were varied are shown alongside cell F3406.

Most neurons were narrowly tuned to the orientation of the luminance gratings (mean circular variance<sup>26</sup> 0.27) and responses were strongly direction selective. This is exemplified in cells F3506 and F3406, which have very low circular variances, and were unresponsive to gratings presented in the null direction. Orientation tuning to the envelope (Fig. 2b) was usually slightly broader than to luminance gratings presented at the cell's optimal spatial and temporal parameters (mean circular variance 0.47), and responses were often less direction selective. In most cases, the luminance gratings were presented at a similar spatial frequency but higher temporal frequency than the envelope. These results support the notion that the processing of the envelope and luminance grating is achieved via neurons with similar spatial characteristics (e.g. as illustrated in the model, the second-stage filter in the nonlinear stream and the luminance filter in the linear stream are similar): the envelope response polar plots (Fig. 2b) were usually very similar to the corresponding luminance polar plots (Fig. 2a). Cell F3506 was unique in that its orientation tuning was sharper to the envelope than to a luminance grating. However, when neurons were tested at their optimal envelope orientation for their responses to different carrier orientations, two striking differences emerged (Fig. 2c): it was rare to find a carrier orientation that produced no response, and orientation tuning was almost always broader than to either the luminance gratings or the envelope. The circular variance for

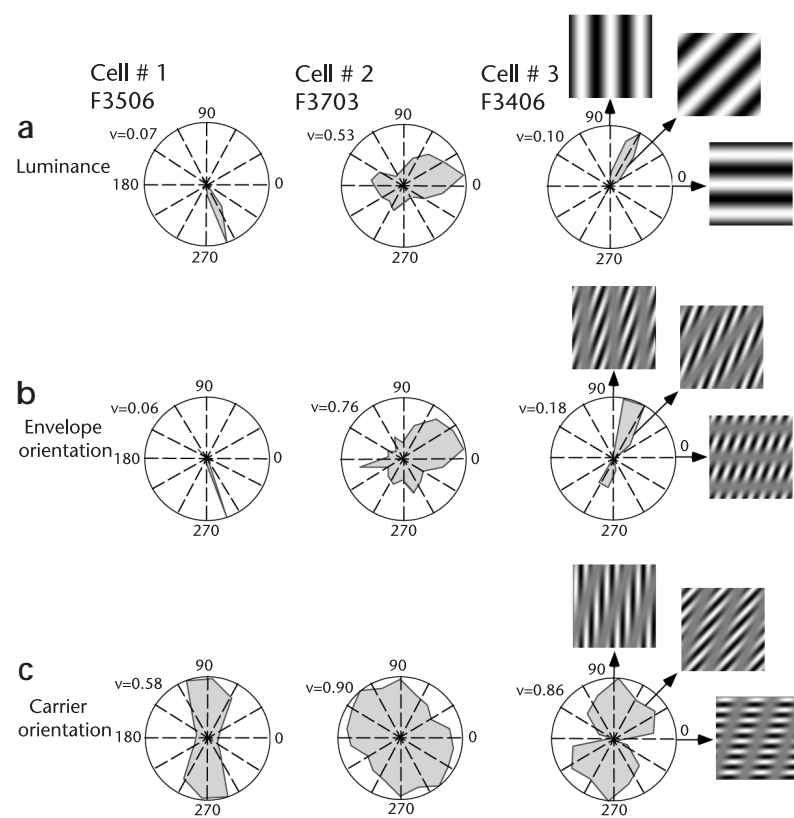


**Fig. 2.** Orientation polar plots for three area 18 neurons. **(a)** Neurons responses to luminance sinewave gratings as a function of orientation. Responses were normalized and spontaneous activity was removed so that non-zero firing rates reflect the neuron's intrinsic tuning. Distance from the origin represents magnitude of response and angular distance represents orientation. Reduced snapshots of the stimuli are shown alongside the rightmost plot, depicting the different stimulus configurations corresponding to different orientations. Indices of circular variance<sup>26</sup> are given above the plots where a value of 1 indicates no tuning (equally responsive across all orientations) and a value of 0 indicates perfectly sharp tuning (responds to only one orientation). **(b)** Responses from the same three neurons to envelope stimuli as a function of the envelope orientation. The orientation of the carrier was set to the optimal orientation measured using luminance sinewave gratings, and envelope orientation varied over 180°. **(c)** Orientation tuning to the carrier. The envelope orientation was fixed at the optimal orientation measured in (b), and carrier orientation was varied over 180°. The degree of orientation selectivity varied across the different cells from relatively sharp tuning (F3506) to broad tuning (F3703). The polar plots are symmetrical in (c) because the carrier is stationary.

these neurons was higher (mean 0.85) because firing rates rarely fell to zero at non-optimal orientations (e.g. the response of cell F3703 only falls to 60% of maximum). The finding of carrier orientation selectivity is important because it is the first physiological demonstration that neurons that process the carrier are oriented, suggesting a cortical locus for the entire nonlinear processing stream.

In order to examine the orientational relationship between the two streams, the optimal orientation of the luminance grating for each neuron was plotted against its optimal envelope orientation (Fig. 3a). The solid line represents the equality ratio (same optimal orientations), whereas the two dashed lines represent orthogonal preferred orientations. The data cluster around the equality line (linear correlation,  $r = 0.88$ ), revealing little variation between a neuron's optimal orientation to the envelope and to a luminance grating of similar spatial frequency. (Note we

report orientation results in order to compare these with the carrier data, which were obtained with a stationary carrier.) Only one neuron showed a difference of more than 45° between its preferred orientations for the two stimuli. In Fig. 3b, the optimal carrier orientation is plotted against the optimal envelope orientation to examine the spatial relationship between the first and second stage filters. The data are highly scattered ( $r = 0.27$ ), indicating that there is no fixed relationship between the optimal carrier and envelope orientations.

#### Discussion

These data unveil two important spatial characteristics of the nonlinear stream: that the neurons that process the carrier are orientation selective (although more broadly so than the neurons that process the envelope), and that there is no fixed relationship between the optimal carrier and optimal envelope

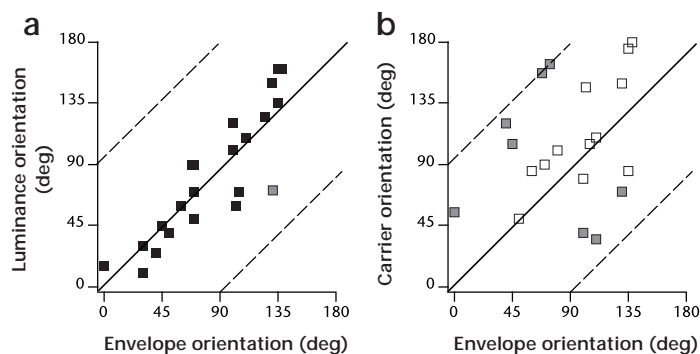


**Fig. 3.** Measured optimal orientations to first- and second-order stimuli. **(a)** Results for 24 neurons, where each point represents one neuron's measured optimal orientation to a luminance sinewave grating (ordinate) against its optimal orientation to the envelope (abscissa). Points in gray represent neurons with an orientational difference between the two parameters greater than 45°. The dashed lines represent orthogonal optimal orientations between the abscissa and ordinate. **(b)** Results for 20 of the neurons shown in (a), but plotting the optimal orientation to the carrier (ordinate) against the optimal orientation to the envelope (abscissa).

orientations. Our results support Model 2, and further imply that there is no rigid orientation combination between the first and second stage filters.

Orientation tuning is widely held to be a cortical property, despite orientational biases being demonstrated in two sub-cortical structures: the lateral geniculate nucleus (LGN)<sup>27–30</sup> and the claustrum<sup>31,32</sup>. In the LGN, however, significant orientational biases only arise when neurons are presented with high spatial frequency stimuli<sup>28,29</sup>. The relatively low degree of orientational biases using physiologically relevant stimuli could only account for some of the carrier-orientation results (e.g. F3703 in Fig. 2). The quite narrow orientation tuning of claustral neurons could potentially account for our carrier orientation results; however, orientation selectivity in the claustrum is thought to result from cortical feedback projections, so that even if the claustrum plays a role in the nonlinear stream, the origin of the orientation selectivity for the carrier would still be predominantly cortical.

The broad carrier tuning indicates that the orientational bandwidth of the first filtering stage is quite large (mean circular variance 0.85). We suggest two neural wiring schemes in the cortex that could produce these broad bandwidths. In the first scheme, broad orientation tuning results directly from broadly oriented first-stage neurons. For example, high-spatial-frequency neurons in layer 4C of area 17<sup>33</sup> could provide the first-stage subunits, which would then be rectified and summed by lower spatial frequency neurons in area 18. Alternatively, the broad orientation tuning might result from the combined inputs of many narrowly tuned, slightly differently oriented, first-stage neurons. Irrespective of the wiring scheme, our results strongly suggest that cortical mechanisms underlie both stages of the nonlinear stream.

We also note the similarity in the preferred orientation to the luminance sinewave grating and the envelope (Fig. 3a). We previously found that the preferred spatial frequency to the envelope was only slightly lower than that to the grating (although the preferred temporal frequency was much lower)<sup>34</sup>. In addition, the preferred direction of motion was the same for first- or second-order stimuli<sup>18</sup>. These results suggest that neurons' responses to these stimuli are invariant in the face of different physical attributes defining the stimulus (form-cue invariance)<sup>11</sup>.

Our results demonstrate that the responses of neurons comprising the nonlinear stream are strongly dependent on the two-dimensional spatial characteristics of the stimulus, suggesting a specialized, selectively tuned cortical mechanism. The lack of a systematic orientation relationship between the carrier and envelope could be functionally important, endowing these neurons with the ability to respond to a broader variety of second-order stimuli, some of which are explicitly defined by orientational differences between the carrier and the envelope (e.g. illusory contours<sup>14,15</sup>). Our results could account for the perception of such stimuli without requiring yet another nonlinear stream with different tuning characteristics.

#### Methods

**ANIMAL PREPARATION.** Acute experiments were carried out on 13 paralyzed adult cats (Gallamine Triethiodide) under nitrous oxide/oxygen anesthesia supplemented with intravenous barbiturate in accordance with the institutional guidelines of McGill University. EEG, EKG, expired CO<sub>2</sub> and body temperature were monitored and maintained at normal levels throughout the experiment. Penetrations were made using platinum-iridium microelectrodes (Frederick Haer) in area 18 because of its higher proportion of envelope responsive neurons. A total of 73 cells were recorded from, of which 33 were envelope responsive, but only 24 could be fully tested on the orientation experiments. Each eye was refract-

ed with a retinoscope, fitted with gas permeable neutral contact lenses, with artificial pupils, and additional spectacle lenses such that stimuli at a viewing distance of 57cm were in focus.

Cells' orientation tuning was quantified by circular variance<sup>26</sup>, a measure of bandwidth for data presented in polar coordinates, defined as:

$$V = 1 - \frac{\left| \sum_k R_k \exp(i2\theta_k) \right|}{\sum_k R_k}$$

where  $R_k$  is the response strength at orientation  $\theta_k$ . A circular variance of 1 indicates no orientation tuning (isotropic response), a variance of 0 reflects perfectly sharp tuning (impulse response).

Cells were classified as envelope responsive if their responses maintained direction selectivity and were tuned to the spatial frequency of the carrier, which was outside the neuron's measured luminance passband. The procedural sequence for envelope measurements was as followed: the optimal carrier spatial frequency was measured first, and then used to measure the optimal envelope spatial and temporal frequencies. The parameters were then set to the above measured optima, and orientation tuning was measured, first to the carrier, then to the envelope.

**STIMULI.** Stimuli were displayed on a NEC XP-17 monitor (frame refresh rate: 67 Hz, raster size: 480 × 480 pixels, mean luminance: 22.3 cd/m<sup>2</sup>). The luminance nonlinearity of the display was measured using a photometer and linearized by gamma-corrected lookup tables. Envelope stimuli were produced as pre-calculated digital movies on a Power Macintosh using Matlab software (The Mathworks) with Videotoolbox<sup>35</sup> and Psychophysics Toolbox<sup>36</sup> software. The carrier spatial frequencies were much higher than the envelope frequencies (ca 10 fold) so that the resultant spectral energy was far outside the neuron's measured luminance-defined passband. The contrast of the luminance sinewave gratings was set to 30%, and that of the envelope stimuli to 70%.

#### Acknowledgements

This work was supported by Canadian MRC (MA 9685) to C.L.B. and an FCAR fellowship to I.M. We are indebted to Steven Dakin for providing comments on this manuscript. We are also grateful to Jingjiang Lei and Lynda Domazet for technical assistance. We also wish to thank Rhone-Poulenc Rorer for their donation of Gallamine Triethiodide.

RECEIVED 11 FEBRUARY; ACCEPTED 29 APRIL 1998.

- Hubel, D.H. & Wiesel, T.N. Functional architecture of macaque visual cortex. *Proc. R. Soc. Lond.* **198**, 1–59 (1977).
- DeValois, R.L., Albrecht, D.G. & Thorell, L.G. Spatial frequency selectivity of cells in macaque visual cortex. *Vision Res.* **22**, 545–559 (1982).
- Spitzer H. & Hochstein, S. Simple- and complex-cell response dependences on stimulation parameters. *J. Neurophysiol.* **53**, 1244–1265 (1985).
- Movshon, J.A., Thompson, I.D. & Tolhurst, D.J. Spatial summation in the receptive fields of simple cells in the cat's striate cortex. *J. Physiol.* **283**, 53–77 (1978).
- DeAngelis, G.C., Ohzawa, I. & Freeman, R.D. Spatiotemporal organization of simple-cell receptive fields in the cat's striate cortex. II Linearity of temporal and spatial summation. *J. Neurophysiol.* **69**, 1118–1135 (1993).
- Adelson, E.H. & Bergen, J.R. Spatiotemporal energy models for the perception of motion. *J. Opt. Soc. Am.* **2**, 284–299 (1985).
- Watson, A.B. & Ahumada, A.J. Model of human visual motion sensing. *J. Opt. Soc. Am.* **2**, 322–342 (1985).
- VanSanten, J.P.H. & Sperling, G. Elaborated Reichardt detectors. *J. Opt. Soc. Am.* **2**, 300–321 (1985).
- Chubb, C. & Sperling, G. Drift-balanced random stimuli: a basis for studying non-Fourier motion perception. *J. Opt. Soc. Am.* **5**, 1986–2006 (1988).
- Cavanagh, P. & Mather, G. Motion: the long and short of it. *Spat. Vis.* **4**, 103–129 (1989).
- Albright, T. Form-cue invariant motion processing in primate visual cortex. *Science* **255**, 1141–1143 (1992).
- Olavarria, J.F., DeYoe, E.A., Knierim, J.J., Fox, J.M. & VanEssen, D.C. Neural responses to visual texture patterns in middle temporal area of the macaque monkey. *J. Neurophysiol.* **68**, 164–181 (1992).
- Zhou, Y.-X. & Baker, C.L. A processing stream in mammalian visual cortex neurons for non-Fourier responses. *Science* **261**, 98–101 (1993).
- Von Der Heydt, R., Peterhans, E. & Baumgartner, G. Illusory contours and cortical neuron responses. *Science* **224**, 1260–1262 (1984).

15. Grosf, D.H., Shapley, R.M. & Hawken, M.J. Macaque V1 neurons can signal "illusory" contours. *Nature* **365**, 550–552 (1993).
16. Derrington, A.M. & Henning, G.B. Linear and non-linear mechanisms in pattern vision. *Current Biol.* **3**, 800–803 (1993).
17. Daugman, J.G. & Downing, C.J. Demodulation, predictive coding, and spatial vision. *J. Opt. Soc. Am.* **4**, 641–660 (1995).
18. Zhou, Y.-X. & Baker, C.L. Envelope-responsive neurons in areas 17 and 18 of cat. *J. Neurophysiol.* **72**, 2134–2150 (1994).
19. Badcock, D.R. & Derrington, A.M. Detecting the displacements of spatial beats : no role for distortion products. *Vision Res.* **29**, 731–739 (1989).
20. Graham, N., Beck, J. & Sutter, A. Nonlinear processes in spatial-frequency channel models of perceived texture segregation: effects of sign and amount of contrast. *Vision Res.* **32**, 719–743 (1992).
21. Wilson, H.R., Ferrera, V.P. & Yo, C. A psychophysically motivated model for two-dimensional motion perception. *Vis. Neurosci.* **9**, 79–97 (1992).
22. Ledgeway, T. & Smith, A.T. Evidence for separate motion-detecting mechanisms for first- and second-order motion in human vision. *Vision Res.* **34**, 2727–2740 (1994).
23. Solomon, J.A. & Sperling, G. Full-wave and half-wave rectification in second-order motion perception. *Vision Res.* **34**, 2239–2257 (1994).
24. Werkhoven, P., Sperling, G. & Chubb, C. Perception of apparent motion between dissimilar gratings: spatiotemporal properties. *Vision Res.* **34**, 2741–2759 (1994).
25. Langley, K., Fleet, D.J. & Hibbard, P.B. Linear filtering precedes nonlinear processing in early vision. *Current Biol.* **6**, 891–896 (1996).
26. Marida, K.V. *Statistics of Directional Data* (Academic Press Inc., London 1972).
27. Vidyasagar, T.R. & Urbas, J.V. Orientation sensitivity of cat LGN neurones with and without inputs from visual cortical areas 17 and 18. *Exp. Brain. Res.* **46**, 157–169 (1982).
28. Vidyasagar, T.R. & Heide, W. Geniculate orientation biases seen with moving sine wave gratings: implications for a model of simple cell afferent connectivity. *Exp. Brain. Res.* **57**, 196–200 (1984).
29. Soodak, R.E., Shapley, R.M. & Kaplan, E. Linear mechanism of orientation tuning in the retina and lateral geniculate nucleus of the cat. *J. Neurophysiol.* **58**, 267–275 (1987).
30. Shou, T. & Leventhal, A.G. Organized arrangement of orientation-sensitive relay cells in the cat's dorsal lateral geniculate nucleus. *J. Neurosci.* **9**, 4287–4302 (1989).
31. Levay, S. & Sherk, H. The visual claustrum of the cat. I. Structure and connections. *J. Neurosci.* **1**, 956–980 (1981).
32. Sherk, H. & Levay, S. The visual claustrum of the cat. III. Receptive field properties. *J. Neurosci.* **1**, 956–980 (1981).
33. Ringach, D.L., Hawken, M.J. & Shapley, R. Dynamics of orientation tuning in macaque primary visual cortex. *Nature* **387**, 281–284 (1997).
34. Mareschal, I. & Baker, C.L. Bandpass temporal and spatial frequency responses to envelopes of second order stimuli in area 18 neurons. *Invest. Ophthalmol. Vis. Sci.* **38**, S624 (1997).
35. Pelli, D.G. The VideoToolbox software for visual psychophysics: Transforming numbers into movies. *Spat. Vis.* **10**, 437–442 (1997).
36. Brainard, D.H. The Psychophysics Toolbox. *Spat. Vis.* **10**, 443–446 (1997).